Journal of Zhejiang University-SCIENCE B (Biomedicine & Biotechnology)
ISSN 1673-1581 (Print); ISSN 1862-1783 (Online)
www.jzus.zju.edu.cn; www.springerlink.com
E-mail: jzus@zju.edu.cn

Novel nano-microspheres containing chitosan, hyaluronic acid, and chondroitin sulfate deliver growth and differentiation factor-5 plasmid for osteoarthritis gene therapy*

Zhu CHEN[§1], Shang DENG[§1,2], De-chao YUAN[1,3], Kang LIU[1], Xiao-cong XIANG[1], Liang CHENG[4], Dong-qin XIAO[1], Li DENG[1], Gang FENG[†‡1]

[1]*Institute of Tissue Engineering and Stem Cells, Nanchong Central Hospital, the Second Clinical Medical College of North Sichuan Medical College, Nanchong 637000, China*

[2]*Department of Orthopedics, Sichuan Provincial Orthopedic Hospital, Chengdu 637000, China*

[3]*Department of Orthopedics, Zigong No. 4 People's Hospital, Zigong 643000, China*

[4]*Department of General Surgery, Chinese Medicine Hospital of Nanchong, Nanchong 637000, China*

[†]E-mail: fenggangncch@163.com

Received Feb. 23, 2018; Revision accepted Aug. 20, 2018; Crosschecked Nov. 21, 2018

Abstract: Objective: To construct a novel non-viral vector loaded with growth and differentiation factor-5 (GDF-5) plasmid using chitosan, hyaluronic acid, and chondroitin sulfate for osteoarthritis (OA) gene therapy. Methods: Nano-microspheres (NMPs) were prepared by mixing chitosan, hyaluronic acid, and chondroitin sulfate. GDF-5 plasmid was encapsulated in the NMPs through electrostatic adsorption. The basic characteristics of the NMPs were observed, and then they were co-cultured with chondrocytes to observe their effects on extracellular matrix (ECM) protein expression. Finally, NMPs loaded with GDF-5 were injected into the articular cavities of rabbits to observe their therapeutic effects on OA in vivo. Results: NMPs exhibited good physicochemical properties and low cytotoxicity. Their average diameter was (0.61±0.20) μm, and encapsulation efficiency was (38.19±0.36)%. According to Cell Counting Kit-8 (CCK-8) assay, relative cell viability was 75%–99% when the total weight of NMPs was less than 560 μg. Transfection efficiency was (62.0±2.1)% in a liposome group, and (60.0±1.8)% in the NMP group. There was no significant difference between the two groups (P>0.05). Immunohistochemical staining results suggested that NMPs can successfully transfect chondrocytes and stimulate ECM protein expression in vitro. Compared with the control groups, the NMP group significantly promoted the expression of chondrocyte ECM in vivo (P<0.05), as shown by analysis of the biochemical composition of chondrocyte ECM. When NMPs were injected into OA model rabbits, the expression of ECM proteins in chondrocytes was significantly promoted and the progression of OA was slowed down. Conclusions: Based on these data, we think that these NMPs with excellent physicochemical and biological properties could be promising non-viral vectors for OA gene therapy.

Key words: Osteoarthritis; Gene therapy; Chitosan; Hyaluronic acid; Chondroitin sulfate; Growth and differentiation factor-5 (GDF-5) plasmid

https://doi.org/10.1631/jzus.B1800095 **CLC number:** R318.08

‡ Corresponding author

§ The two authors contributed equally to this work

* Project supported by the National Natural Science Foundation of China (No. 81201407), the Bureau of Science & Technology and Intellectual Property Nanchong City (Nos. NSMC20170203 and NSMC20170310), the Health and Family Planning Commission of Sichuan Province (No. 17JP496), and the Research Projects of North Sichuan Medical College (No. CBY13-A-ZD09), China

ORCID: Gang FENG, https://orcid.org/0000-0002-2814-4319

1 Introduction

Osteoarthritis (OA) is the most common disease of movable joints, and primarily affects the knees, hips, and hands. It is estimated that 10%–20% of the population worldwide is affected by OA. Its main features are articular cartilage degradation, inflammation of the synovial membrane, and sclerosis of subchondral bone associated with the formation of osteophytes (Vinatier et al., 2016). Studies have shown that aging, hormonal dysregulation, and other factors prevent infiltration and diffusion of nutrients into the matrix and cause accumulation of waste, leading to chondrocyte death and dissolution of the matrix (Piera-Velazquez et al., 2002). Current therapies for OA focus on pain management, viscosupplementation (via intra-articular injections of hyaluronic acid), and joint replacement (Robinson et al., 2016). However, these therapies address only the symptoms, not the underlying disease etiology, and fail to prevent cartilage damage and degradation of other joint tissues. With the identification of new pathogenic mechanisms of OA in recent years, novel therapeutic strategies can now be developed to inhibit the processes that drive OA pathology. For instance, gene therapy could be used to modify the relevant OA-related genes. Cell therapy and tissue-engineered cartilage could be used to repair injured articular cartilage. These novel therapeutic strategies are now gradually being introduced into clinical practice (Adachi et al., 2006; Madry and Cucchiarini, 2016; Jevotovsky et al., 2018).

Currently, various growth factors, cytokines, and matrix metalloproteinases are the common molecular targets of OA therapies (Alcaraz et al., 2010). Growth and differentiation factor-5 (GDF-5) is a member of the transforming growth factor-β (TGF-β) superfamily and bone morphogenetic protein (BMP) family that regulate cell growth and differentiation. Previous studies indicated that GDF-5 plays an important role in the formation of cartilage and articular cavities. Exogenous application of the GDF-5 protein or gene may promote the differentiation of bone and cartilage (Coleman et al., 2011). In a preliminary study, we found that adipose-derived stem cells were successfully induced to form cartilage cells by the introduction of a GDF-5 plasmid. The induced adipose-derived stem cells could secrete chondrocyte extracellular matrix (ECM), glycosaminoglycans (GAGs), collagen II, and aggrecan (Feng et al., 2008). In another study, we transfected degenerating nucleus pulposus cells with a GDF-5 plasmid. GDF-5 transfection improved the growth of the cells and promoted the expression of ECM proteins (Luo et al., 2016). These two studies indicated that GDF-5 can effectively induce the formation of chondrocytes and regulate the expression of ECM proteins in chondrocytes. Thus, GDF-5 might slow down articular cartilage degradation and provide a new treatment strategy for OA.

Because of its inherent biocompatibility and biodegradability, chitosan (CS) is a promising tool for several biological and medical applications, especially as a non-viral gene vector (Bravo-Anaya et al., 2016). Due to its positive charge, CS can easily penetrate the negatively charged cell membrane and bind to negatively charged genes to protect them against degradation by nucleases (Bor et al., 2016; Ramesh Kumar et al., 2016). Furthermore, its ability to escape the endosome increases transfection efficiency and minimizes off-target effects (Zhang et al., 2016). Also, its *N*-acetyl-glucosamine and glucosamine monomers are natural components of cartilage, which have been proven to be chondroprotective (Lu et al., 2014). Based on this evidence, CS maybe an ideal gene therapy vector for OA. In recent years, new functional groups have been introduced into CS to improve its therapeutic functions, including improvements to its biocompatibilty, transfection efficiency, and target delivery. In the case of OA, hyaluronic acid sodium (HA) and chondroitin sulfate (CHS), components of the chondrocyte ECM, are widely used in the clinic to treat OA, with notable therapeutic benefits. Research shows that HA and CHS can diminish inflammation, cushion forces that impact joints, and lubricate diseased joints (Abate et al., 2010; McAlindon et al., 2012). In some studies, delivery of HA and CHS therapy with CS produced excellent outcomes. For instance, when nanoparticles were prepared with CS and HA for gene silencing, inclusion of HA enhanced the biocompatibility and transfection efficiency of the nanoparticles (Al-Qadi et al., 2013). Kaderli et al. (2015) used a hydrogel prepared with CS and HA to treat OA. The hydrogel had good biocompatibility and did not produce acute clinical signs of pain or inflammation. CHS has also been employed as a

coating agent to increase the stability and transfection efficiency of a plasmid DNA (pDNA)/CS complex (Hagiwara et al., 2012). These findings indicate that a combination of HA, CHS, and CS may be a more suitable gene therapy vector for OA treatments.

In this study, we aimed to prepare nanomicrospheres (NMPs) with CS, HA, and CHS as a vector to deliver a GDF-5 plasmid for gene therapy treatment of OA. This non-viral vector was used to transfer the GDF-5 plasmid into chondrocytes. NMPs were injected into rabbits to observe their effects on OA. In this way, we aimed to prepare a novel non-viral vector better suited for gene therapy of OA and specific for OA.

2 Materials and methods

2.1 Preparation of NMPs with CS, HA, and CHS loaded with GDF-5 plasmid

NMPs were prepared by mixing CS, HA, CHS, and GDF-5 plasmid at 55 °C using electrostatic adsorption. Briefly, 250 mg low molecular weight CS (Sigma, USA) was dissolved in 10 ml deionized water, and then 62.5 mg HA from *Streptomyces hyalurolyticus* (Aladdin, China) and 31.25 mg CHS from shark cartilage (Sigma, USA) were added and mixed together to form the material solution. The resulting solution was sterilized by filtering through a 0.22-μm filter (Millipore, USA) and incubated at 55 °C for 1 h. GDF-5 plasmid (20 μl) solution (1 mg/ml) was transferred to a 1-ml sterile tube and warmed to 55 °C for 60 s. Next, the two solutions were immediately added into the same tube at a ratio of 20:1 (N/P). The resulting mixture was shaken using a vortex oscillator (Thmorgan VM100, USA) at maximum speed for 2 min, and then incubated for 30 min at room temperature. Finally, the NMPs were collected by centrifugation, washed three times with deionized water, and stored at −20 °C.

2.2 Basic characteristics of GDF-5 plasmid-loaded NMPs

NMPs were suspended in deionized water and their size distribution was examined with a laser diffraction particle size analyzer (Horiba LA 920, Japan). A drop of microsphere solution was pipetted onto a clear metal stub and sputter-coated with gold after the solution dried at room temperature. NMP morphology was observed using a scanning electron microscope (FEI Quanta 200, the Netherlands).

The lyophilized microsphere powder was tableted with potassium bromide. The sample was observed at room temperature using a Fourier transform infrared (FTIR) spectrometer (Nicolet 5700, USA). FTIR spectrograms of CS, HA, and CHS were also created under the same conditions.

NMPs were separated by centrifugation at 1000*g* for 5 min and washed three times with deionized water. The liquid supernatant was collected and its absorbance measured at 280 nm using an ultraviolet spectrophotometer (Shimadzu UV-1800, Japan). The NMPs were dried until they reached a constant weight, which was recorded. The encapsulation efficiency (EE) and loading efficiency (LE) were calculated using the following formulas:

$$EE=(W_1-W_2)/W_3\times100\%,$$
$$LE=(W_1-W_2)/W_1\times100\%,$$

where W_1, W_2, and W_3 are the weights of total plasmid, plasmid in the liquid supernatant, and total nanomicrospheres, respectively.

Combination of the plasmid and NMPs was determined by gel electrophoresis. Different NMP solutions and pure GDF-5 plasmid were tested by 0.8% (8 g/L) gel electrophoresis at 80 V for 40 min (Bio-Rad, Power Pac Universal Power Supply, USA) and viewed using a gel documentation system (Bio-Rad, ChemiDoc, USA).

2.3 Release of GDF-5 plasmid

Lyophilized NMP powder (5 mg) was resuspended with 10 ml phosphate-buffered solution (PBS) (pH 7.4). The suspensions were shaken at 100 r/min at 37 °C. The buffer (500 μl) was collected at a predetermined time point and then 500 μl of buffer was supplied. The plasmid content was measured at 280 nm by ultraviolet spectrophotometry. The amounts of plasmid released were calculated using the following formula: accumulated released ration=plasmid amount in buffer/total plasmid amount×100%.

2.4 Cytotoxicity assays

All rabbits were provided by the Experimental Animals Center of North Sichuan Medical College

(Nanchong, China). The experimental protocol was approved by the Institution's Animal Care and Use Committee (The Second Clinical Medical College of North Sichuan Medical College, No. 2016-(shen)-11). New Zealand white rabbits (female, average weight (2.5±0.5) kg) were sacrificed with overdose pentobarbital sodium, and articular cartilage was collected. Cartilage was digested by 0.2% collagenase II at 37 °C for 12–16 h. Chondrocytes were collected by centrifugation at 400*g* for 5 min and cultured in Dulbecco's modified Eagle medium (DMEM; Hyclone, USA) supplemented with 10% fetal bovine serum (FBS; Gibco, USA) at 37 °C and 5% CO_2. The medium was changed every three days. Cells were digested with 0.25% trypsin for passaging when cell confluence reached 80%–90%.

Chondrocytes (1×10^4, Passage 1) were cultured in 96-well plates with DMEM containing 20% FBS. When cell confluence reached about 80%–90%, different weights of NMPs were added and cultured with the cells for 48 h. Then the medium was changed and the cells were washed with PBS (pH 7.2–7.4) three times. Cell proliferation was measured using Cell Counting Kit-8 (CCK-8; Dojindo, Japan). Test solutions were prepared by diluting the stock solution at a ratio of 1:10 (v/v) in cell culture medium. Test solutions (200 μl) were added to each well and incubated for 2 h. Then 100 μl of test solution was transferred to another 96-well plate for measurement at 450 nm (Cytation 3, Biotek, USA). Chondrocytes cultured without NMPs were used as the control group.

2.5 Cell transfection of NMPs loading GFP plasmid

To check the cell transfection result directly, a green fluorescent protein (GFP) plasmid was encapsulated into NMPs. The preparation method was the same as that described above. Chondrocytes (100 μl, 1×10^5 ml^{-1}, Passage 1) were cultured with 10% FBS at 37 °C and 5% CO_2 in 24-well plates. The medium was changed to DMEM without serum and antibiotics when cell confluence reached about 80%–90%. NMPs containing 2 μg GFP plasmid were incubated with 50 μl DMEM without serum or antibiotics at 25 °C for 15 min and then cultured with cells for 72 h. Liposome 2000 was used for the positive group. Five microliters of liposome 2000 (Biyutian, China) and 2 μg of GDF-5 plasmid were mixed with 20 and 50 μl DMEM (without serum or antibiotics), respectively. Next, liposome 2000 and plasmid were mixed together and incubated at 25 °C for 15 min and cultured with cells. After 6 h, the transfection reagent was discarded and the medium was changed to DMEM containing 10% FBS. NMPs loaded with null plasmid were used as a negative control to account for effects of DNA transfection. Null-plasmid NMPs were transfected according to the same procedure as used for GFP-plasmid NMPs. Cells cultured with normal medium acted as an additional negative control group. The cells were observed using a light microscope (Wanheng XDS1, China). Green fluorescence was observed after 72 h using a fluorescence microscope (Nikon TS100, Japan) and the transfection results were evaluated in the different groups. Propidium iodide (4 μmol/L; AAT Bioquest, USA) was used to stain dying cell nuclei at 37 °C for 5 min before green fluorescence was observed. All observations were performed in triplicate for each group, with five fields selected in every well. Cell number and green fluorescent cell number were counted using ImageJ. Transfection efficiency was estimated using the following formula: transfection efficiency=green fluorescent cell number/cell number×100%. Representative figures are reported.

2.6 Chondrocyte ECM histology evaluation

To evaluate the effect of NMPs on chondrocyte ECM, chondrocytes were transfected with NMPs loaded with GDF-5 plasmid. The transfection method was the same as that described above. The medium was changed 72 h after transfection and changed again every two days. After one week, specific ECM protein expression was detected by collagen II immunohistochemical staining and aggrecan immunfluorescence staining.

Immunochemical staining for collagen II was performed using a collagen staining kit (Chondrex, USA) according to the manufacturer's instructions. The cells were colored by incubating cells with 3,3'-diaminobenzidine (DAB) substrate solution for 3 min and were then observed under a light microscope (Wanheng XDS1, China). The immunochemical method used for staining for aggrecan was similar to that used for staining collagen II. Cells were treated with 3% hydrogen peroxide for 30 min at 25 °C and blocked with diluted sheep serum (10 μl in 200 μl 5% bovine serum albumin (BSA) solution) for 15 min at

37 °C. Then cells were incubated with rabbit anti-mouse aggrecan polyclonal antibody (1:200; Thermo, USA) for 12–18 h at 4 °C, followed by incubation with goat anti-mouse fluoresceinisothiocynate (FITC)-conjugated secondary antibody (1:200; Molecular Probes, USA) and 4',6-diamidino-2-phenylindole (DAPI, 1:1000; Biosharp, China) for 1 h at 25 °C in a moist dark box. Finally, cells were observed under a fluorescence microscope.

2.7 Chondrocyte ECM biochemical assays

To analyse the expression of chondrocyte ECM accurately, the GAG and hydroxyproline (hypro) content were measured. Chondrocytes were cultured for one week after transfection and the cells were collected for biochemical assays. The assay method was as previously reported (Liu et al., 2015). Briefly, cells were digested and then washed with PBS three times for further assay. Cell number was determined by quantification of total DNA content. The DNA was extracted using a DNA kit (Omega Bio-tek, USA), according to the manufacturer's instructions. The quantification of total DNA content was determined using the Hoechst 33258 (Sigma-Aldrich, St. Louis, MO, USA) fluorometric dye assay with calf thymus DNA as a standard. The sulfated GAG (sGAG; Sigma-Aldrich, St. Louis, MO, USA) content of the samples was measured using a modified dimethylmethylene blue colorimetric assay (21 mg 1,9-dimethylmethylene blue in 5 ml absolute ethanol and 2.0 g sodium formate, volume-adjusted to 800 ml with distilled water, and pH-adjusted to 1.5 with formic acid), using CHS as the standard. The hypro content was determined after hydrolysis of the cells in 6 mol/L HCl for 24 h at 110 °C using the dimethylaminobenzaldehyde (Sigma Aldrich, St. Louis, MO, USA) colorimetric assay. For each assay, all cells and standards were processed in quintuplicate. The sGAG/DNA and hypro/DNA ratios were calculated for each group.

2.8 Effect of NMP treatment on a rabbit model of OA

The relevant experiments about rabbit protocol were declared as described above, and ethics were conformed to relevant rules.

OA model rabbits were created using the classic Hulth method (Hulth et al., 1970). Briefly, rabbits were anesthetized by injection of 30 mg/kg pentobarbital sodium and the knee joints were opened via a lateral parapatellar skin incision. Next, the anterior cruciate ligament and medial collateral ligament were cut off and the medial meniscus was completely resected. The wound was washed with sterile physiological saline. Then the joint was carefully returned to its original site and layer sutured. All rabbits were given a single injection of 1 200 000 U benzathine benzylpenicillin and were allowed to move freely without fixing the lesioned limb. The ten model rabbits were divided into two groups randomly. In the experimental group, 100 μl of NMPs containing 5 μg GDF-5 were injected into the knee joint one week after the operation and then every two days for one week. The rabbits in the saline negative control group were injected with 100 μl of saline at the same time points. Rabbits that did not undergo surgery comprised the no OA control group. There were five rabbits in each group. Rabbits were housed one per cage, and could access water and chow ad libitum.

All rabbits were sacrificed four weeks after the operation with overdose pentobarbital sodium. The knee joints were harvested and photographed to evaluate the degree of OA, based on the morphology of the joint. Then a piece of tissue in the lesion site was collected for ECM biochemical assays using the method described above. Finally, the knee joints were fixed in 4% paraformaldehyde for one day and demineralized in decalcifying solution for at least ten days. Demineralized joints were then embedded in paraffin and cut into 5-μm sections. The sections were dewaxed in xylene, followed by hematoxylin and eosin (H&E) staining and immunohistochemical staining to compare the degree of OA pathology between different groups. H&E staining was performed according to standard H&E staining procedures and immunohistochemical staining procedures were performed as described above.

2.9 Statistical analysis

All the staining experiments were performed in triplicate. Representative photos were taken. The other quantitative experiments were performed in quintuplicate. Averaged values are expressed as mean±standard deviation (SD). Statistical evaluation was performed by chi-square test. A P-value of less than 0.05 was considered significant.

3 Results

3.1 Basic characteristics of NMPs loaded with GDF-5 plasmid

In this study, we successfully prepared NMPs with CS, HA, and CHS, loaded with GDF-5 plasmid (Fig. 1a). The NMPs had a spherical morphology (Fig. 1a) and an average diameter of (0.61±0.20) μm. The encapsulation efficiency was (38.19±0.36)% and the loading efficiency was (0.72±0.05)%. As shown in Fig. 1b, the electrophoretic band of the NMPs appeared in the sample well, which suggested that the plasmid was encapsulated in the NMPs, not only adhering to the surface of the microspheres.

Because the NMPs were formed by electrostatic adsorption between chitosan and the plasmid, further tests were needed to demonstrate that the NMPs contained HA and CHS. To test for the presence of HA and CHS, dried NMP powder was assayed using FTIR spectroscopy. HA and CHS are both glucuronic acids, with characteristic carboxyl and amide groups, and are notably different from CS. A moderate-intensity characteristic absorption peak could be observed at 1310–1200 cm^{-1} (Fig. 1c) caused by the stretching vibration of the C–N bond and the bending vibration of N–H bond. Compared with HA and CHS, CS produces only weak characteristic absorption peaks at this wavelength. Therefore, this peak can be used to detect the presence of HA and CHS independently of CS. This peak could be found in the FTIR analysis of NMPs (Fig. 1c), which indicated that the NMPs contained HA and CHS.

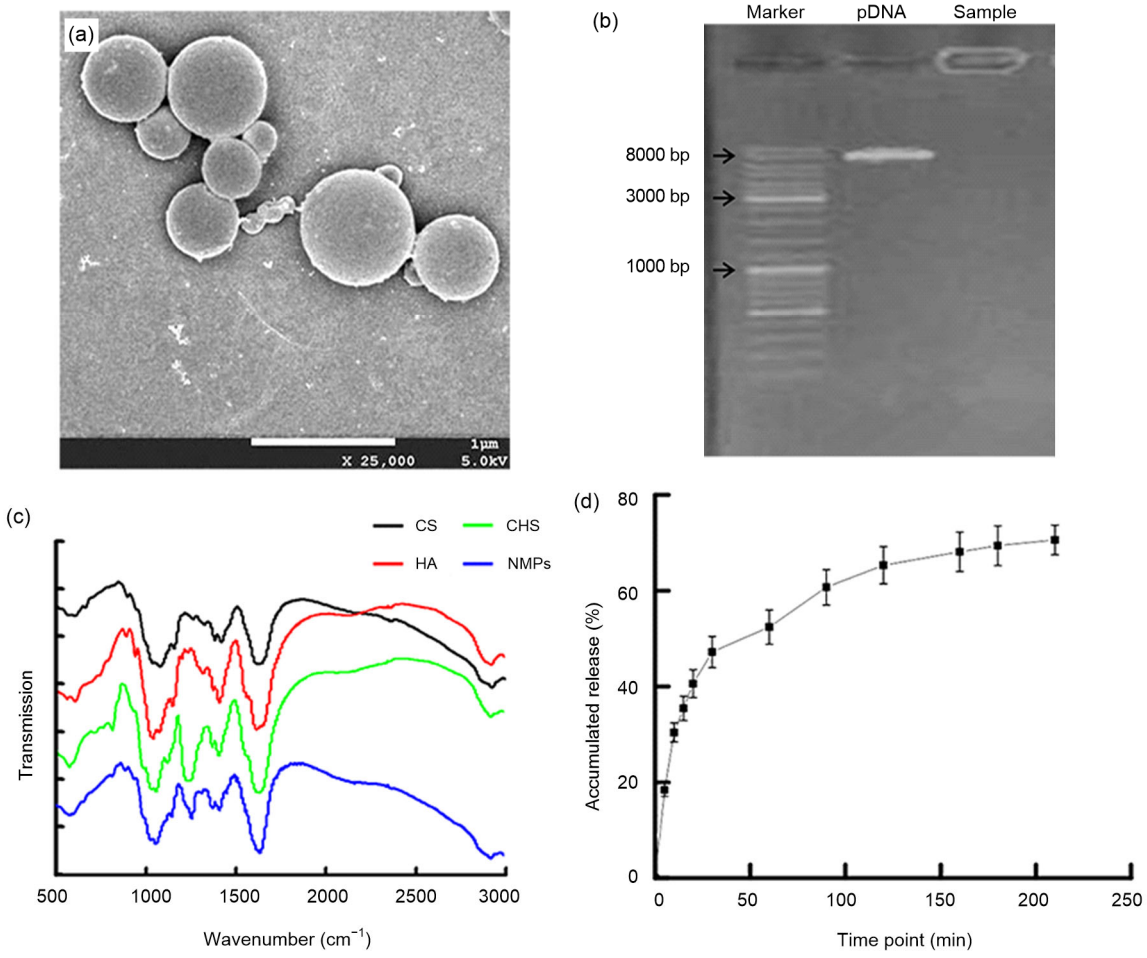

Fig. 1 Basic characteristics of NMPs loaded with GDF-5 plasmid

(a) The morphology of microspheres as shown by scanning electron microscopy (×25000, bar=1 μm); (b) Agarose electrophoresis gel showing the encapsulation of the plasmid in microspheres; (c) Fourier transform infrared (FTIR) test of nanomicrospheres (NMPs); (d) The plasmid release in phosphate-buffered solution (PBS) (pH 7.4). Data are expressed as mean± standard deviation (SD) (n=3). CS: chitosan; HA: hyaluronic acid sodium; CHS: chondroitin sulfate

The GDF-5 plasmid was released from NMPs in PBS (Fig. 1d). The plasmid was rapidly released from NMPs within 40 min of the fast dissolution of HA and CHS. With the dissolution of HA and CHS, the structure of NMPs was broken up, and the plasmid was quickly released from NMPs. However, at 180 min the accumulated release of plasmid had stabilized at only about 70%. This may have been because of the residual ionic bond formed by electrostatic adsorption between CS and the plasmid.

3.2 Cytotoxicity

To choose a suitable dosage for transfection experiments and to determine if NMPs are cytotoxic, we measured the cytotoxicity of different amounts of NMPs using CCK-8. Relative cell viability decreased with increasing NMP concentration (Fig. 2). Relative cell viability was 75%–99% when the total weight of NMPs was less than 560 μg, but decreased to less than 40% when the total weight of NMPs was greater than 2240 μg. The relative cell viabilities in groups A, B, and C were significantly different from those of the other groups (P<0.05).

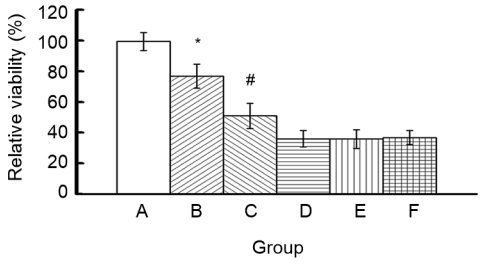

Fig. 2 Cytotoxicity of NMPs

Groups: A, 280 μg NMPs (2 μg plasmid DNA (pDNA)); B, 560 μg NMPs (4 μg pDNA); C, 1120 μg NMPs (8 μg pDNA); D, 2240 μg NMPs (16 μg pDNA); E, 5600 μg NMPs (40 μg pDNA); F, 11200 μg NMPs (80 μg pDNA). Data are expressed as mean±SD (n=3). * P<0.05 groups A vs. B; # P<0.05 groups B vs. C

3.3 Cell transfection in vitro

The GFP plasmid was encapsulated into the NMPs to observe the transfection result directly. The null plasmid group was the negative group and the liposome group was the positive group. Green fluorescence could be observed 48 h after transfection in the liposome group and NMP group (Figs. 3b and 3c). Results showed that the number of fluorescent cells and their fluorescence intensity were similar between the two groups. From analysis using ImageJ, the calculated transfection efficiency was (62.0±2.1)% in liposome group and (60.0±1.8)% in NMP group. There was no significant difference between the two groups (P>0.05). There was no obvious fluorescence in the null plasmid group (Fig. 3b).

In the next experiment, we measured the effect of NMP treatment on the chondrocyte ECM by examining two specific ECM proteins, collagen II and aggrecan. Only a few cells expressed collagen II in the untreated control group and the null plasmid-NMP group (Fig. 4). However, the number of collagen II-positive cells increased significantly in the liposome group and the NMP group after treatment. Liposome-mediated and NMP-mediated transfections increased collagen II-positive cells to a similar degree, indicating that the two vectors had similar transfection efficiency. Aggrecan staining produced results similar to those from collagen II staining (Fig. 5). Together, these immunolabeling results showed that treatment with NMPs-loaded with GDF-5 can promote ECM protein secretion in chondrocytes, at least to some extent. Analysis of the biochemical composition of chondrocyte ECM supported this result (Figs. 4e and 5e). Hypro and GAG, indicators of collagen II and aggrecan, respectively, were measured one week after transfection. The hypro/DNA ratio was 9.82±0.19 in the control group and 15.31±0.22 in the NMP group, and the GAG/DNA ratio was 5.71±0.31 in the control group and 9.72±0.21 in the NMP group. These results showed that the hypro and GAG contents in the liposome group and NMP group markedly increased compared with the other two groups (P<0.05).

3.4 Effect of NMP treatment on a rabbit model of OA

After the operation, all rabbits remained in good condition. Acute inflammatory reaction on the wound was gradually relieved by daily disinfection and the injection of antibiotics. No rabbits died and no obvious adverse reactions were reported. All rabbits were included in the statistical analysis as planned. At four weeks, obvious osteophytes were formed and the cartilage ruptured in the saline control group. Obvious deformities could be observed in the right femoral condyle and the cartilage was visibly abraded in the

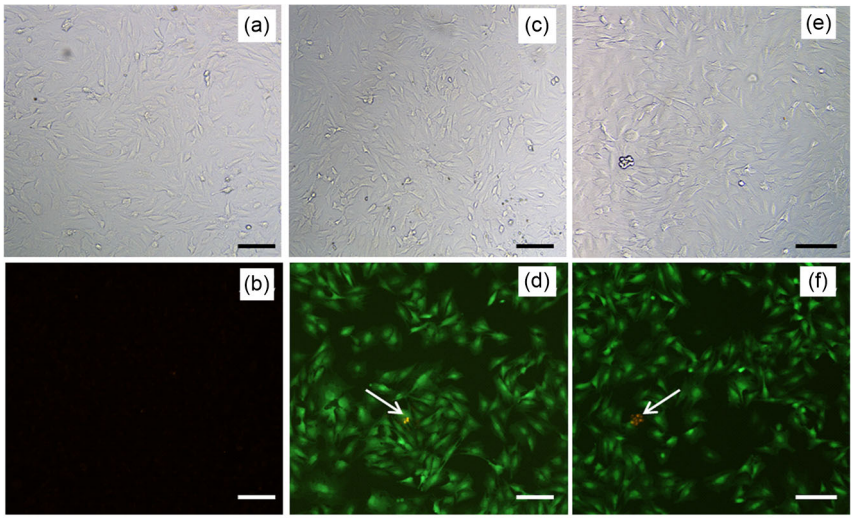

Fig. 3 Transfection results for chondrocytes with green fluorescent protein (GFP) plasmid (×100, bar=25 μm)

(a, b) Null plasmid group; (c, d) Liposome group; (e, f) NMPs group; (a, c, e) Cells were observed by microscope; (b, d, f) Cells were observed by fluorescence microscope. Green fluorescence represents the green fluorescence protein, and red fluorescence (arrow) represents dying cells (Note: for interpretation of the references to color in this figure legend, the reader is referred to the web version of this article)

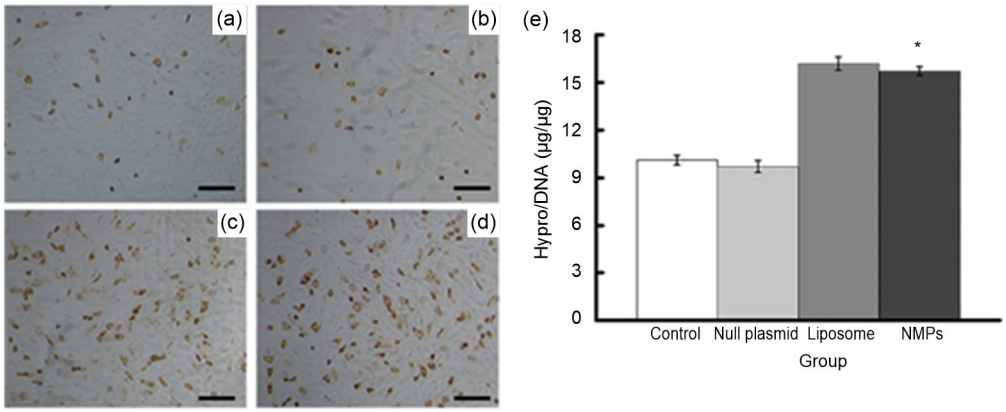

Fig. 4 Expression of collagen II after transfection

(a–d) Immunohistochemical staining results (×100, bar=25 μm): (a) control group; (b) null plasmid group; (c) liposome group; (d) NMPs group. (e) Quantification of hydroxyproline (hypro) deposited in chondrocytes using hypro assay. Data are expressed as mean±SD (n=5). * P<0.05 vs. the control group

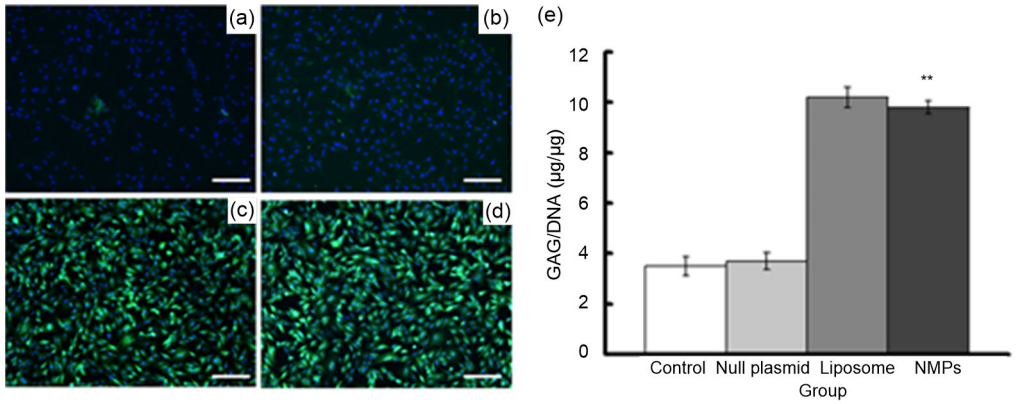

Fig. 5 Expression of aggrecan after transfection

(a–d) Immunohistochemical staining results (×100, bar=25 μm): (a) control group; (b) null plasmid group; (c) liposome group; (d) NMPs group; green fluorescence represents extracellular matrix (ECM), blue fluorescence represents the cell nucleus. (e) Quantification of glycosaminoglycan (GAG) deposited in chondrocytes using GAG assay. Data are expressed as mean±SD (n=5). ** P<0.01 vs. the control group (Note: for interpretation of the references to color in this figure legend, the reader is referred to the web version of this article)

left femoral condyle (Fig. 6a). Based on the formation of osteophytes, the OA was in stages 2–3 according to the Kellgren-Lawrence (K-L) grading method (Kellgren and Lawrence, 1957). H&E staining showed that the anatomical structure of the joints was obviously changed in the saline control group. The hyaline cartilage was completely transformed into fibrous cartilage. The tidal line disappeared, resulting in no obvious boundary between the cartilage and subchondral bone. Furthermore, hyperplastic tissue could be observed in the cartilage layer (Fig. 7a). Finally, collagen II immunohistochemical staining showed that the section was nearly negative for collagen II expression. Due to the poorer specificity of aggrecan expression, aggrecan labeling could be observed in the saline control group, but the intensity was significantly lower than that in the no OA control group (Figs. 8a and 8b). Based on the injury to the cartilage, the OA was in stages 1–2 according to the articular cartilage damage scoring system of the International Cartilage Repair Society (ICRS) (van den Borne et al., 2007).

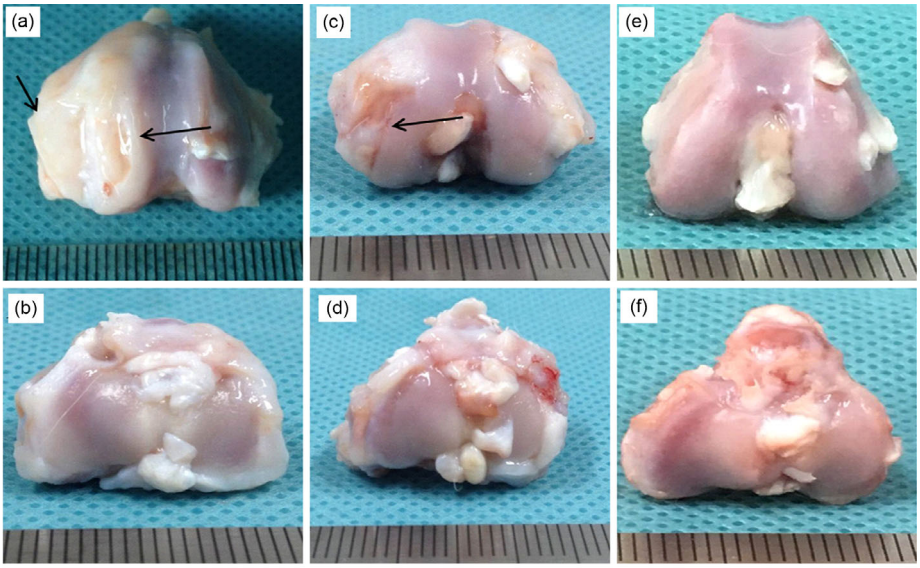

Fig. 6 Gross morphology of the knee joints of OA model rabbits four weeks after NMP injection
(a, b) Saline control group; (c, d) NMP group; (e, f) No osteoarthritis (OA) control group; (a, c, e) Femoral condyle; (b, d, f) Tibial plateau. Sites of injury are indicated by the arrows

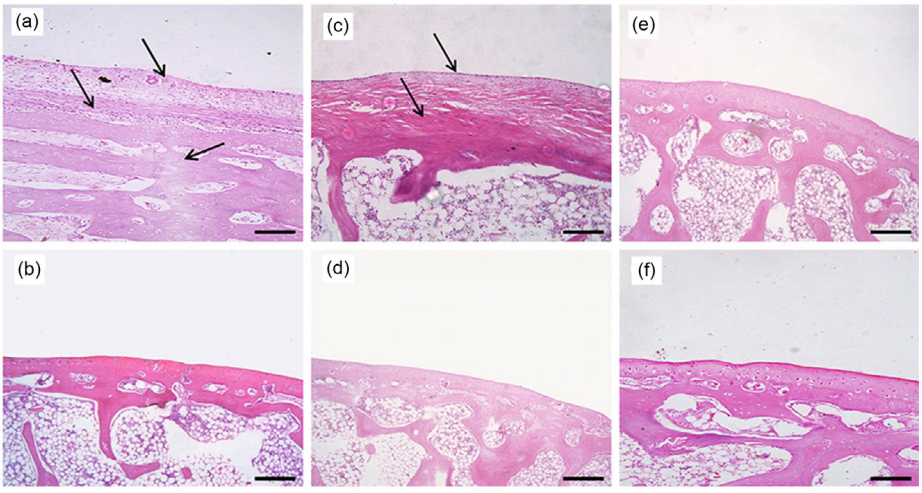

Fig. 7 H&E staining of the knee joints of OA model rabbits four weeks after NMP injection (×40, bar=100 μm)
(a, b) Saline control group; (c, d) NMP group; (e, f) No osteoarthritis (OA) control group; (a, c, e) Femoral condyle; (b, d, f) Tibial plateau. Sites of injury are indicated by the arrows

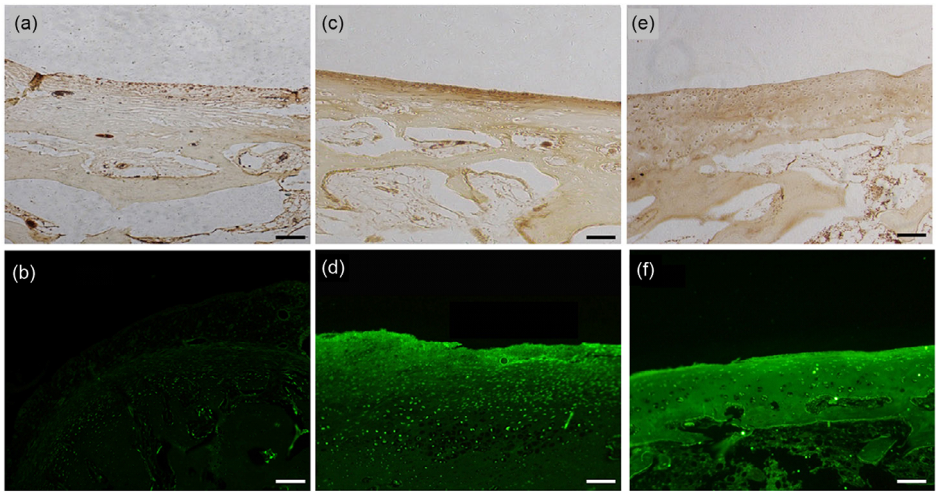

Fig. 8 Immunohistochemical staining results of the knee joints of OA model rabbits four weeks after NMP injection (×40, bar=100 μm)
(a, b) Saline control group; (c, d) NMP group; (e, f) No osteoarthritis (OA) control group; (a, c, e) Collagen II immunohistochemical staining; (b, d, f) Aggrecan immunofluorescence staining

Cartilage damage was obviously less extensive in the NMP-treated group relative to the saline control group. Although there were still some cracks on the articular surface, the structure was mostly intact and the major cartilage remained smooth and shiny (Fig. 6c).

Based on the formation of osteophytes, the OA was in stages 0–1 according to the K-L grading method. As shown in the H&E staining results, tissue clearance increased in the upper hyaline cartilage, which indicated that the tissue was dropsical to some extent. Although some hyaline cartilage was slowly transformed into fibrous cartilage, most retained its normal characteristics. Some of the subchondral bone vasculature invaded the hyaline cartilage layer, but the overall structure of the cartilage was still complete (Fig. 7c). As shown by the immunohistochemistry results, although the cartilage structure was altered to some extent, the expression of the ECM proteins collagen II and aggrecan was higher in the NMP-treated group than in either the saline or the no surgery control group (Fig. 8). This demonstrated that our NMP treatment stimulated the growth of the ECM in chondrocytes. Based on injury to the cartilage, the OA was in stages 0–1 according to the ICRS scale.

Note that gross cartilage morphology and H&E staining showed no obvious differences in the tibial plateau among the three groups, which suggested that the tibial plateau was not affected in this model of OA (Figs. 6 and 7). For this reason, we do not report immunohistochemical staining results for the tibial plateau.

4 Discussion

Articular cartilage is an avascular and neural tissue consisting mainly of water (>70%) and two major organic components: collagen II and aggrecan. Highly crosslinked collagen II fibrils form an organized network that traps negatively charged proteoglycan aggregates and interacts with other collagens, small proteoglycans, and other cartilage-specific and nonspecific matrix proteins (Goldring and Goldring, 2016). The physical properties of articular cartilage are determined by two components: (1) the fibrillar collagen network that provides tensile strength, and (2) the entrapped proteoglycan aggregates that provide compressive resilience (Andriacchi and Favre, 2014; Guo et al., 2015). The early pathological changes that occur in OA increase water content and cartilage matrix degradation. Damage to the collagen network changes the physiological environment and mechanical characteristics of joints, which is followed by sequential osteochondral changes in the joint (Robinson et al., 2016).

In this study, GDF-5 was chosen as a therapeutic gene, because it can effectively promote secretion of

ECM in chondrocytes. Recently, GDF-5 has been widely used in the treatment of musculoskeletal diseases, especially intervertebral disc and cartilage diseases. Bucher et al. (2013) successfully transfected mesenchymal stem cells with GDF-5 by electroporation. Mesenchymal stem cells expressed GDF-5 for up to 21 d. The two markers for chondrogenesis and a marker of discogenesis were all upregulated. Murphy et al. (2015) reported that GDF-5 could promote the expression of one or more markers of chondrocytes in human dedifferentiated chondrocytes . Feng et al. (2008) and Luo et al. (2016) showed that GDF-5 could promote the expression of collagen II and aggrecan, the two marker of chondrocytes, in adipose-derived stem cells and degenerating nucleus pulposus cells. Increased expression of collagen II and aggrecan can help maintain the structure of the collagen network and inhibit the sequential osteochondral changes, to some extent. Next, we prepared a novel non-viral gene therapy vector: GDF-5-loaded NMPs with CS, HA, and CHS. Clearly, safety is an essential factor that determines whether or not a gene vector can be used for clinical applications (Kumar et al., 2016; Lukashev and Zamyatnin, 2016). Viral vectors have high transfection efficiency, but cannot be widely used in the clinic, due to controversy surrounding their safety. Specifically, there is evidence that suggests viral vectors could increase immunogenicity and mutagenicity. For these reasons, other non-viral vectors have been developed, including liposomes, polyethylene polyimide, and polylysine (Carrillo et al., 2014; Majzoub et al., 2016). CS is a common natural cationic polymer. It can be used as a non-viral vector, due to its cell membrane penetrability, ability to escape the endosome, and targeting capabilities. HA can enhance transfection efficiency for chondrocytes because cell-surface glycoprotein 44 (CD44) acts as the primary cell surface receptor for HA internalization and turnover (Lu et al., 2011). In OA, due to stimulation by inflammatory factors (such as interleukin 1 (IL-1)), CD44 receptors are highly expressed and easily detected (Chow et al., 1995). The presence of HA in the nanoparticles could allow HA-containing nanoparticles to gain facilitated access to the target cells via a receptor-mediated endocytosis pathway. In this study, the transfection efficiency of NMPs was similar to that of liposome 2000. This may have been because HA improves the internalization of the nanoparticles with the chondrocytes. More importantly, HA and CHS regulate cell growth and differentiation, and have anti-inflammatory effects. They are both widely used in clinical treatment of OA. In this study, the introduction of HA and CHS into the vector may have directly improved degradation of the chondrocyte ECM and relieved the symptoms of OA before the GDF-5 plasmid produced therapeutic effects. Thus, HA and CHS enabled the non-viral vector itself to have some therapeutic effects on OA, making it much more suitable for delivery of gene therapy treatments for OA.

Our results indicated that the GDF-5 plasmid-loaded NMPs were prepared successfully (Fig. 1). The NMPs have low cytotoxicity, according to the results of the CCK-8 assays (Fig. 2). The data showed that relative cell viability was 95% when 280 μg of NMPs were added to cell cultures. When 560 μg of NMPs were added, the ratio remained relatively high (75%). According to the cytotoxic grading standard in the *United States Pharmacopeia*, this level of cytotoxicity is classed as grade one, which means that the treatment could be applied clinically. The cytotoxicity increased with the NMP content. The relative viability was below 40% when the content reached 2240 μg (16 μg plasmid) (Fig. 2). Given the low cytotoxicity of the raw materials and the use of no cytotoxic chemical agents in all preparation procedures, we think that the cytotoxicity observed was mainly attributable to the concentration difference in the culture medium after the addition of the NMPs. In the transfection experiments, the NMPs loaded GFP plasmid directly, as shown by the high efficiency of transfection, which was similar to that achieved with liposome (Fig. 3). Based on these data, NMPs may be an excellent non-viral vector.

In our study, further in vitro transfection experiments showed that the expression of collagen II and aggrecan was significantly increased after co-culture with NMPs loaded with GDF-5 plasmid (Figs. 4 and 5). This result indicated that ECM protein expression was significantly enhanced in chondrocytes. When NMPs loaded with GDF-5 plasmid were injected into animals with OA, cartilage morphology and the structure of the affected joints were significantly improved relative to those of the saline control group. In the NMP group, we observed characteristics that are typical of early OA: a relatively smooth and

shiny articular surface of the fermoral condyle, swelling of the cartilage matrix, and the development of surface fibrillations. In contrast, the saline control group had obvious osteophytes and a disordered anatomical structure, suggesting that OA had progressed further in these animals (Figs. 6 and 7). This conclusion was further verified by immunohistochemistry staining for the chondrocyte-specific ECM proteins collagen II and aggrecan (Fig. 8). Based on these results, we conclude that NMPs can effectively promote the expression of ECM proteins in chondrocytes and slow down the progression of OA.

5 Conclusions

In this study, NMPs loaded with GDF-5 plasmid were successfully prepared with CS, HA, and CHS. These NMPs had spherical morphology, uniform size, and low cytotoxicity. The addition of HA and CHS had therapeutic effects on OA. When these novel gene vectors were injected into lesioned joints, HA and CHS might begin to work before the GDF-5 plasmid was expressed. Pain could be relieved and symptoms could improve quickly. Later, expression of GDF-5 from the plasmid could effectively and continuously promote the expression of ECM proteins in chondrocytes. After NMP treatment, we found that OA symptoms were obviously relieved and the progress of OA was slowed down in vivo. In summary, these NMPs have excellent characteristics that make them a promising gene therapy vector for treatment of OA.

Contributors

Zhu CHEN performed the experimental research and data analysis, wrote and edited the manuscript. Shang DENG, De-chao YUAN, Kang LIU, Xiao-cong XIANG, and Li DENG performed biological experimental research. Liang CHENG performed the establishment of animal models. Dong-qin XIAO performed the relevant microsphere experimental research. Gang FENG contributed to the study design, data analysis, writing and editing of the manuscript. All authors read and approved the final manuscript and, therefore, had full access to all the data in the study and take responsibility for the integrity and security of the data.

Compliance with ethics guidelines

Zhu CHEN, Shang DENG, De-chao YUAN, Kang LIU, Xiao-cong XIANG, Liang CHENG, Dong-qin XIAO, Li DENG, and Gang FENG declare that they have no conflict of interest.

All institutional and national guidelines for the care and use of laboratory animals were followed.

References

Abate M, Pulcini D, di Iorio A, et al., 2010. Viscosupplementation with intra-articular hyaluronic acid for treatment of osteoarthritis in the elderly. *Curr Pharm Des*, 16(6):631-640. https://doi.org/10.2174/138161210790883859

Adachi N, Ochi M, Deie M, et al., 2006. Lateral compartment osteoarthritis of the knee after meniscectomy treated by the transplantation of tissue-engineered cartilage and osteochondral plug. *Arthroscopy*, 22(1):107-112. https://doi.org/10.1016/j.arthro.2005.10.019

Alcaraz MJ, Megías J, García-Arnandis I, et al., 2010. New molecular targets for the treatment of osteoarthritis. *Biochem Pharmacol*, 80(1):13-21. https://doi.org/10.1016/j.bcp.2010.02.017

Al-Qadi S, Alatorre-Meda M, Zaghloul EM, et al., 2013. Chitosan-hyaluronic acid nanoparticles for gene silencing: the role of hyaluronic acid on the nanoparticles' formation and activity. *Colloids Surf B Biointerfaces*, 103:615-623. https://doi.org/10.1016/j.colsurfb.2012.11.009

Andriacchi TP, Favre J, 2014. The nature of in vivo mechanical signals that influence cartilage health and progression to knee osteoarthritis. *Curr Rheumatol Rep*, 16(11):463. https://doi.org/10.1007/s11926-014-0463-2

Bor G, Mytych J, Zebrowski J, et al., 2016. Cytotoxic and cytostatic side effects of chitosan nanoparticles as a non-viral gene carrier. *Int J Pharm*, 513(1-2):431-437. https://doi.org/10.1016/j.ijpharm.2016.09.058

Bravo-Anaya LM, Soltero JFA, Rinaudo M, 2016. DNA/chitosan electrostatic complex. *Int J Biol Macromol*, 88:345-353. https://doi.org/10.1016/j.ijbiomac.2016.03.035

Bucher C, Gazdhar A, Benneker LM, et al., 2013. Nonviral gene delivery of growth and differentiation factor 5 to human mesenchymal stem cells injected into a 3D bovine intervertebral disc organ culture system. *Stem Cells Int*, 2013:326828. https://doi.org/10.1155/2013/326828

Carrillo C, Suñé JM, Pérez-Lozano P, et al., 2014. Chitosan nanoparticles as non-viral gene delivery systems: determination of loading efficiency. *Biomed Pharmacother*, 68(6):775-783. https://doi.org/10.1016/j.biopha.2014.07.009

Chow G, Knudson CB, Homandberg G, et al., 1995. Increased expression of CD44 in bovine articular chondrocytes by catabolic cellular mediators. *J Biol Chem*, 270(46):27734-27741. https://doi.org/10.1074/jbc.270.46.27734

Coleman CM, Scheremeta BH, Boyce AT, et al., 2011. Delayed fracture healing in growth differentiation factor 5-deficient mice: a pilot study. *Clin Orthop Relat Res*,

469(10):2915-2924.
https://doi.org/10.1007/s11999-011-1912-0

Feng G, Wan YQ, Balian G, et al., 2008. Adenovirus-mediated expression of growth and differentiation factor-5 promotes chondrogenesis of adipose stem cells. *Growth Factors*, 26(3):132-142.
https://doi.org/10.1080/08977190802105917

Goldring SR, Goldring MB, 2016. Changes in the osteochondral unit during osteoarthritis: structure, function and cartilage-bone crosstalk. *Nat Rev Rheumatol*, 12(11): 632-644.
https://doi.org/10.1038/nrrheum.2016.148

Guo HQ, Maher SA, Torzilli PA, 2015. A biphasic finite element study on the role of the articular cartilage superficial zone in confined compression. *J Biomech*, 48(1): 166-170.
https://doi.org/10.1016/j.jbiomech.2014.11.007

Hagiwara K, Nakata M, Koyama Y, et al., 2012. The effects of coating pDNA/chitosan complexes with chondroitin sulfate on physicochemical characteristics and cell transfection. *Biomaterials*, 33(29):7251-7260.
https://doi.org/10.1016/j.biomaterials.2012.06.040

Hulth A, Lindberg L, Telhag H, 1970. Experimental osteoarthritis in rabbits. Preliminary report. *Acta Orthop Scand*, 41(5):522-530.
https://doi.org/10.3109/17453677008991540

Jevotovsky DS, Alfonso AR, Einhorn TA, et al., 2018. Osteoarthritis and stem cell therapy in humans: a systematic review. *Osteoarthrit Cartil*, 26(6):711-729.
https://doi.org/10.1016/j.joca.2018.02.906

Kaderli S, Boulocher C, Pillet E, et al., 2015. A novel biocompatible hyaluronic acid-chitosan hybrid hydrogel for osteoarthrosis therapy. *Int J Pharm*, 483(1-2):158-168.
https://doi.org/10.1016/j.ijpharm.2015.01.052

Kellgren JH, Lawrence JS, 1957. Radiological assessment of osteo-arthrosis. *Ann Rheum Dis*, 16(4):494-502.
https://doi.org/10.1136/ard.16.4.494

Kumar SR, Markusic DM, Biswas M, et al., 2016. Clinical development of gene therapy: results and lessons from recent successes. *Mol Ther Methods Clin Dev*, 3:16034.
https://doi.org/10.1038/mtm.2016.34.eCollection 2016

Liu K, Chen Z, Luo XW, et al., 2015. Determination of the potential of induced pluripotent stem cells to differentiate into mouse nucleus pulposus cells *in vitro*. *Genet Mol Res*, 14(4):12394-12405.
https://doi.org/10.4238/2015.October.16.6

Lu HD, Zhao HQ, Wang K, et al., 2011. Novel hyaluronic acid-chitosan nanoparticles as non-viral gene delivery vectors targeting osteoarthritis. *Int J Pharm*, 420(2): 358-365.
https://doi.org/10.1016/j.ijpharm.2011.08.046

Lu HD, Dai YH, Lv LL, et al., 2014. Chitosan-graft-polyethylenimine/DNA nanoparticles as novel non-viral gene delivery vectors targeting osteoarthritis. *PLoS ONE*, 9(1):e84703.
https://doi.org/10.1371/journal.pone.0084703

Lukashev AN, Zamyatnin AA Jr, 2016. Viral vectors for gene therapy: current state and clinical perspectives. *Biochemistry (Mosc)*, 81(7):700-708.
https://doi.org/10.1134/S0006297916070063

Luo XW, Liu K, Chen Z, et al., 2016. Adenovirus-mediated GDF-5 promotes the extracellular matrix expression in degenerative nucleus pulposus cells. *J Zhejiang Univ-Sci B (Biomed & Biotechnol)*, 17(1):30-42.
https://doi.org/10.1631/jzus.B1500182

Madry H, Cucchiarini M, 2016. Gene therapy for human osteoarthritis: principles and clinical translation. *Expert Opin Biol Ther*, 16(3):331-346.
https://doi.org/10.1517/14712598.2016.1124084

Majzoub RN, Ewert KK, Safinya CR, 2016. Cationic liposome-nucleic acid nanoparticle assemblies with applications in gene delivery and gene silencing. *Philos Trans A Math Phys Eng Sci*, 374(2072):20150129.
https://doi.org/10.1098/rsta.2015.0129

McAlindon TE, Driban JB, Lo GH, 2012. Osteoarthritis year 2011 in review: clinical. *Osteoarthritis Cartilage*, 20(3): 197-200.
https://doi.org/10.1016/j.joca.2011.12.015

Murphy MK, Huey DJ, Hu JC, et al., 2015. TGF-β1, GDF-5, and BMP-2 stimulation induces chondrogenesis in expanded human articular chondrocytes and marrow-derived stromal cells. *Stem Cells*, 33(3):762-773.
https://doi.org/10.1002/stem.1890

Piera-Velazquez S, Jimenez SA, Stokes DG, 2002. Increased life span of human osteoarthritic chondrocytes by exogenous expression of telomerase. *Arthrit Rheum*, 46(3): 683-693.
https://doi.org/10.1002/art.10116

Ramesh Kumar D, Saravana Kumar P, Gandhi MR, et al., 2016. Delivery of chitosan/dsRNA nanoparticles for silencing of wing development vestigial (*vg*) gene in *Aedes aegypti* mosquitoes. *Int J Biol Macromol*, 86:89-95.
https://doi.org/10.1016/j.ijbiomac.2016.01.030

Robinson WH, Lepus CM, Wang Q, et al., 2016. Low-grade inflammation as a key mediator of the pathogenesis of osteoarthritis. *Nat Rev Rheumatol*, 12(10):580-592.
https://doi.org/10.1038/nrrheum.2016.136

van den Borne MPJ, Raijmakers NJH, Vanlauwe J, et al., 2007. International Cartilage Repair Society (ICRS) and Oswestry macroscopic cartilage evaluation scores validated for use in Autologous Chondrocyte Implantation (ACI) and microfracture. *Osteoarthritis Cartilage*, 15(12): 1397-1402.
https://doi.org/10.1016/j.joca.2007.05.005

Vinatier C, Merceron C, Guicheux J, 2016. Osteoarthritis: from pathogenic mechanisms and recent clinical developments to novel prospective therapeutic options. *Drug Discov Today*, 21(12):1932-1937.
https://doi.org/10.1016/j.drudis.2016.08.011

Zhang XQ, Zhang H, Yin LQ, et al., 2016. A pH-sensitive nanosystem based on carboxymethyl chitosan for tumor-targeted delivery of daunorubicin. *J Biomed Nanotechnol*,

12(8):1688-1698.
https://doi.org/10.1166/jbn.2016.2278

中文概要

题　目：携载生长分化因子 5 质粒的壳聚糖-透明质酸-硫酸软骨素微球在骨关节炎基因治疗中的应用

目　的：骨关节炎是临床上的一种常见病和多发病。本研究尝试利用壳聚糖、透明质酸和硫酸软骨素为载体，制备一种携载生长分化因子 5（GDF-5）质粒的纳米微球用于骨关节炎的基因治疗。

创新点：首次利用壳聚糖、透明质酸、硫酸软骨素三种原料制备可携载 GDF-5 质粒的三元纳米微球，并将其应用到骨关节炎的治疗中。

方　法：在 55 °C 下，按不同比例混合壳聚糖、透明质酸钠、硫酸软骨素和 GDF-5 质粒，利用静电吸附原理制备携载 GDF-5 质粒的三元纳米微球。分别利用扫描电镜和激光粒度散射仪测试微球的形貌和粒径；利用凝胶电泳检测质粒与微球的结合情况；利用 CCK-8 检测微球的细胞毒性。将携载 GDF-5 质粒的微球与软骨细胞共培养，并将脂质体和空载组作为对照组，在预定的时间点通过免疫荧光染色、免疫组化染色以及生化成分分析，观察微球对软骨细胞外基质分泌情况的影响。最后将该纳米微球注射到骨关节炎模型兔体内，通过大体观察、苏木精-伊红（H&E）染色、免疫荧光染色和免疫组化分析该微球对骨关节炎的作用。

结　论：本研究成功地利用壳聚糖、透明质酸和硫酸软骨素为原料，制备出携载 GDF-5 质粒的纳米微球。其中 GDF-5 质粒可以有效地促进软骨细胞外基质的分泌，透明质酸和硫酸软骨素是临床上常见的治疗骨关节炎的药物。微球具有良好的理化性能，其细胞毒性小，转染效率高，在体内外均能有效地促进软骨细胞外基质的分泌，能够在一定程度上延缓骨关节炎的进展。该纳米微球将是一种极具希望的可应用于骨关节炎基因治疗的载体。

关键词：骨关节炎；基因治疗；三元微球；GDF-5 质粒